ATP Analogs and Muscle Contraction: Mechanics and Kinetics of Nucleoside Triphosphate Binding and Hydrolysis

M. Regnier, D. M. Lee, and E. Homsher
Department of Physiology, School of Medicine, University of California, Los Angeles, California 90095 USA

ABSTRACT The mechanical behavior of skinned rabbit psoas muscle fiber contractions and in vitro motility of F-actin (V_f) have been examined using ATP, CTP, UTP, or their 2-deoxy forms (collectively designated as nucleotide triphosphates or NTPs) as contractile substrates. Measurements of actin-activated heavy meromyosin (HMM) NTPase, the rates of NTP binding to myosin and actomyosin, NTP-mediated acto-HMM dissociation, and NTP hydrolysis by acto-HMM were made for comparison to the mechanical results. The data suggest a very similar mechanism of acto-HMM NTP hydrolysis. Whereas all NTPs studied support force production and stiffness that vary by a factor 2 or less, the unloaded shortening velocity (V_u) of muscle fibers varies by almost 10-fold. 2-Deoxy ATP (dATP) was unique in that V_u was 30% greater than with ATP. Parallel behavior was observed between V_f and the steady-state maximum actin-activated HMM ATPase rate. Further comparisons suggest that the variation in force correlates with the rate and equilibrium constant for NTP cleavage; the variations in V_u or V_f are related to the rate of cross-bridge dissociation caused by NTP binding or to the rate(s) of product release.

INTRODUCTION

Muscular work results from the cyclic interaction between actin and myosin in which chemical energy, derived from the hydrolysis of MgATP, is converted into mechanical work, force, and shortening (chemomechanical transduction). Myosin and acto-myosin ATPase activity have been studied extensively in solution, and a number of steps have been identified and characterized (reviewed in Homsher and Millar, 1990). In muscle fibers, however, the orderly array of thin and thick filaments may impose steric and strain-dependent constraints on acto-myosin interactions. Recently, measurements of force transients after quick length changes or the photolysis of caged compounds (such as ATP, ADP, P_i, and Ca^{2+}) have been used to determine 1) which cross-bridge transition steps occur during muscle fiber contractions, and 2) the strain-dependent properties of these cross-bridge steps. Several chemomechanical models now exist, most of which can be incorporated into the following simplified scheme:

In this model ATP binds to the myosin S1 (M) of an attached (rigor) cross-bridge (step 1), followed rapidly by the dissociation of actin (A) from M (step 2), producing the detached M · ATP cross-bridge state. After hydrolysis of the γ-phosphate (step 3), a low-force, weakly bound A~M · ADP · P_i state can form (step 4), which is in a rapid equilibrium with the M · ADP · P_i state. During isometric contractions the cross-bridge then isomerizes to a strongly bound state (step 5) that produces strain, resulting in force generation (denoted by *). Studies of the tension transients following caged-P_i photolysis and pressure jumps have been interpreted as indicating that this strongly bound, high strain state occurs before and is rapidly stabilized by the release of P_i (step 6) from the cross-bridge (Fortune et al., 1991; Dantzig et al., 1992; Millar and Homsher, 1992; Walker et al., 1992). In the isometric contraction this is followed by the slower release of ADP from the cross-bridge (step 7) at the end of the power stroke.

$$\begin{array}{ccccccccc} & & 1 & & & & 5 & 6 & 7 \\ \mathrm{AM^*} + \mathrm{ATP} & \leftrightarrow & \mathrm{AM \cdot \mathit{ATP}} & \rightleftharpoons & \mathrm{A \sim M \cdot ADP \cdot P_i} & \leftrightarrow & \mathrm{AM^* \cdot ADP \cdot P_i} & \leftrightarrow \mathrm{AM^* \cdot ADP} \leftrightarrow \mathrm{AM^*} & \text{attached} \\ & & 2\downarrow\uparrow & & 3 \quad \uparrow\downarrow 4 & & & & \\ & & \mathrm{A + M \cdot ATP} & \leftrightarrow & \mathrm{A + M \cdot ADP \cdot P_i} & & & & \text{detached} \end{array}$$

Scheme 1

While Scheme 1 accounts for much of the experimental data from fibers, it is not a complete solution, as it cannot adequately describe fiber force and shortening under a variety of conditions and does not include any strain-dependent transitions. Regnier et al. (1995), for example, demonstrated that force generation (step 5 in Scheme 1) may occur as a two-step process, consisting of a Ca^{2+}-regulated transition from the weakly bound, low-force A~M · ADP · P_i state to an intermediate, strongly bound, low-force

Received for publication 28 February 1997 and in final form 16 March 1998.

Address reprint requests to Dr. Earl Homsher, Physiology Department, Center for Health Sciences, UCLA, Los Angeles, CA 90024. Tel.: 310-825-6976; Fax: 310-206-6551; E-mail: ehomsher@physiology.medsch.ucla.edu.

Dr. Regnier's present address is Center for Bioengineering, School of Medicine, University of Washington, Seattle, WA 98195-7962.

0006-3495/98/06/3044/15 $2.00

AM · ADP · P_i state that precedes myosin isomerization to the force-exerting AM*·ADP·P_i state. Furthermore, there is strong evidence that release of ADP from the cross-bridge is a two-step process in muscle fibers (Bagshaw and Trentham, 1975; Sleep and Hutton, 1980; Dantzig et al., 1991). Recently Homsher et al. (1997) have provided evidence that the forward rate constant for the force-generating isomerization (step 5) varies with fiber shortening velocity and is thus strain-dependent.

Another method used to study the chemomechanical process in muscle fibers is to substitute analogs of ATP (NTPs) as the substrate for contraction. Correlation of the mechanical behavior in NTPs with changes in rate constants of steps in the hydrolysis may provide useful information about mechanically and energetically important steps. Some of these analogs (e.g., ITP, GTP, and aza-ATP) bind more slowly to myosin, support less force and shortening velocity, and have slower steady-state hydrolysis rates than when MgATP is the substrate for contraction (Pate et al., 1991, 1993; White et al., 1993). Two notable exceptions to this are 2-[(4-azido-2-nitrophenyl)amino]ethyltriphosphate (MgNANTP) (which behaves in a manner similar to that of MgATP; Pate et al., 1991) and MgCTP, which support similar force and a slower shortening velocity, but are reported to have a faster steady-state hydrolysis rate than MgATP (Pate et al., 1993). Both NANTP and MgCTP exhibit a sensitivity to ADP and P_i concentrations similar to that seen with ATP (Pate et al., 1991). Furthermore, Shimizu et al. (1991) showed that deoxy forms of ATP support translocation of F-actin over myosin-coated coverslips in motility assays at speeds similar to that of ATP and have a higher turnover rate by HMM, in the absence and presence of actin.

In the present study we extended this work by surveying several naturally occurring NTPs (dATP, CTP, dCTP, UTP, dUTP, ITP, and GTP) to find substrates that support a variety of force levels and shortening speeds as a prelude to experiments examining the posthydrolytic steps of the actomyosin ATPase cycle. Similar to previous work (Pate et al., 1993; White et al., 1993), we found that at 6 mM most of the NTPs surveyed reduced isometric force, fiber stiffness, and unloaded velocity of shortening (V_u) in muscle fibers and slowed F-actin filament sliding velocity (V_f) in the in vitro motility assay. In contrast, dATP produces the same isometric force as ATP, but both V_u and V_f were increased by ~30%. We then selected dATP, CTP (which produces similar isometric force but slows V_u by ~50%), and UTP (which reduces isometric force by ~50% and slows V_u by 80%) for a more detailed study of their effects on muscle mechanics and the kinetic steps in NTP binding and hydrolysis. In this paper we characterize the cross-bridge steps most likely to limit the ability of fibers to shorten. In the companion paper (Regnier et al., 1997) we characterize the cross-bridge steps (the posthydrolysis steps) that control steady-state force, the kinetics of force generation, and the strain dependency of cross-bridge cycling in muscle fibers. Preliminary reports of this work were published previously (Regnier et al., 1993; Regnier and Homsher, 1996; Homsher et al., 1993).

MATERIALS AND METHODS

Fiber solutions

All fiber solutions were at 200 mM ionic strength (pH 7.1, 10°C) and, for control measurements, contained 100 mM *N*,*N*-bis(2-hydroxyethyl)-2-aminoethane sulfonic acid (BES), 6 mM MgATP, 1 mM Mg^{2+} (added as magnesium acetate), 20 mM K-acetate, 20 mM EGTA (as K-EGTA for relaxation solution or CaEGTA for activation solution), 15 mM creatine phosphate, and 200-4000 units ml^{-1} creatine phosphokinase (Sigma, St. Louis, MO). In preactivation solutions, the K-EGTA concentration was reduced to 2 mM, and 18 mM HDTA was added to maintain a total concentration of (EGTA + HDTA) at 20 mM. For comparison of substrates, MgATP was replaced with MgCTP, MgUTP, MgITP, MgGTP, or the Mg2-deoxy forms of ATP (dATP), CTP (dCTP), and UTP (dUTP). For nucleotide concentrations, the stocks were scanned using the following extinction coefficients and wavelengths: ATP, 15.4×10^3 M^{-1} cm^{-1} (259 nm); dATP, 15.4×10^3 M^{-1} cm^{-1} (259 nm); CTP, 9.1×10^3 M^{-1} cm^{-1} (271 nm); UTP, 8.1×10^3 M^{-1} cm^{-1} (261 nm); ITP 12.2×10^3 M^{-1} cm^{-1} (249 nm); GTP 13.7×10^3 M^{-1} cm^{-1} (252 nm). In some experiments the NTP concentration [NTP] was increased or decreased, and the K-acetate concentration was adjusted to maintain ionic strength at 200 mM. Contaminant levels of nucleotide diphosphates (NDPs) in activation solutions were determined by high-performance liquid chromatography (HPLC) (Waters Associates, Milford, MA; Partisil 10 SAX, 4.6 mm [I.D.] × 250 mm steel column, Whatman, Clifton, NJ). The mobile phase, 0.4 M $NH_4H_2PO_4$ (pH 4.0), was pumped through the column at 3 ml min^{-1}. The elutant's optical density was monitored at 254 nm. ATP stocks contained <1% contamination with ADP. NTP stocks contained 1–3% contamination by NDPs and were free of ATP contamination. Several stock solutions were further purified by chromatography on a DEAE-52 column equilibrated with 10 mM tetraethyl ammonium bicarbonate (TEAB) at pH 7.4 and elution with a 10–700 mM gradient. The NTP peak fractions were pooled and rotary evaporated three times at 25°C with methanol washes between rotary evaporation. This process reduced NDP + NMP contamination to <1%. The results (maximum isometric force and unloaded shortening velocity) obtained using the column-purified NTP were not different from those using the original stocks. This result suggests that the levels of NDP and P_i contamination of the NTP samples were not significant to the results obtained. To determine the ability of the creatine phosphokinase (CPK) (1–20 mg/ml) to regenerate NTP from NDP, activation solutions were prepared with 5 mM NDP in place of NTP. To start the reaction, CPK was added to the activation solution (at 10°C), and, at progressive times, samples were taken and the reaction was stopped by the addition of 5 N HCl. The solutions were brought to pH 4.0 by the addition of NaOH, and then injected onto the HPLC for determination of the time course of NTP synthesis. These measurements showed that ATP and dATP were completely rephosphorylated within 20 s, but CTP and UTP gave only 48% and 51% rephosphorylation after 30 min in 20 mg CPK/ml. Nevertheless, CPK at 20 mg/ml was added to CTP and UTP containing fiber solutions to mitigate increases in the basal NDP concentration.

Fiber preparation and mechanical measurements

Bundles of psoas muscle fibers from female New Zealand White rabbits were harvested, chemically skinned by the glycerol extraction method (Goldman et al., 1984), stored at −20°C, and used for up to 6 weeks. Several times, freshly skinned fibers were used after incubation in a relaxation solution containing 0.1% Triton for 15 min after to the experiment. Procedures for mounting short lengths of single fibers (3–5 mm), changing solutions, and making mechanical measurements were as previously described (Dantzig et al., 1992). After mounting, laser diffraction was used to set sarcomere spacing at 2.8 μm. Measurements of fiber width

(w) and depth (d) were made with a compound microscope (400×) from three separate locations along the fiber length, and an average cross-sectional area was computed ($w \cdot d \cdot [\pi/4]$). Force transients were acquired by digitizing signals at 20 kHz and were analyzed using the program KFIT (Millar and Homsher, 1990). Fibers were excluded if the control level of isometric force decreased by >10% during the experiment. Unloaded shortening velocity (V_u) was measured using the "slack test" (Edman, 1979). The reported V_u values are expressed in muscle lengths per second (ML/s) (the observed shortening velocity (mm/s divided by the muscle length, corresponding to a sarcomere length of 2.25 μm). The apparent maximum V_u (max V_u) and the apparent K_m (K_{app}) were obtained from measurements of V_u over a range of NTP concentrations (from 100 μM to 12 mM), and using least-squares linear regression of the 1/NTP versus $1/V_u$. Fiber stiffness was measured as the change in force per length, using sinusoidal length changes of 0.05–0.1% of fiber length (peak to peak) at 0.5 kHz. Stiffness values are reported as a percentage of stiffness in control activation solution (6 mM ATP, pCa 4.5).

Protein preparation

Rabbit skeletal myosin was prepared from white back muscles (Margossian and Lowey, 1982) and used immediately or stored for up to 4 weeks, as previously described (Homsher et al., 1992). Heavy meromyosin (HMM) was produced by digestion of myosin by α-chymotrypsin for 10 min at 25°C (Toyoshima et al., 1987). Actin was prepared according to the method of Eisenberg and Keilly (1974) and was labeled with phalloidin-tetramethylrhodamine (Molecular Probes, Eugene, OR), according to the method of Kron and Spudich (1986) for motility experiments. Protein concentrations were determined by measuring absorption at 280 nm with extinction coefficients of 0.53, 0.60, and 1.15 $ml \cdot mg^{-1} \cdot cm^{-1}$ for myosin, HMM, and actin, respectively.

In vitro motility assays

Assay conditions, techniques, and measurement procedures for f-actin filament sliding speed (V_f) were as described in Homsher et al. (1992). All measurements of V_f were made at 25°C, and motility solutions contained 25 mM KCl, 25 mM 3-(*N*-morpholino)propanesulfonic acid (MOPS) (pH 7.4), 2 mM $MgCl_2$, 2 mM K_2EGTA, 1 mM Na_2-NTP, and a glucose (3 mM)/glucose oxidase (27 units/ml)/catalase (260 units/ml) system to slow photobleaching. Total ionic strength was computed as 54 mM, and in experiments in which the MgNTP was raised or lowered, [KCl] concentration was diminished or raised to maintain ionic strength. At 6 mM MgNTP, 1 mM Mg^{2+}, and 0 mM KCl, the ionic strength of motility solutions was 56 mM.

Measurement of the kinetics of NTP binding, cleavage, and hydrolysis

The proteins used in these experiments were dialyzed overnight against the solutions to be used in the transient kinetic and steady-state NTPase measurements. The steady-state rate of NTP hydrolysis was measured using a colorimetric phosphate procedure (based on the formation of phosphomolybdate) (White, 1982) from five time points for HMM alone and in the presence of increasing actin concentrations ranging from 0 to 20 μM. The solutions contained 10 mM MOPS (pH 7.1 at 10°C and 7.4 at 25°C), 3 mM $MgCl_2$, 2 mM K_2EGTA, 1 mM dithiothreitol (DTT), and 1 mM Na_2-NTP (ionic strength 20–23 mM), and were thermostatted in a temperature bath at 10°C or 25°C (ionic strength 20–23 mM). The reactions were initiated by the addition of NTP. Estimations of the maximum hydrolysis rate of NTP (k_{cat}) and K_m were obtained from least-squares linear fits to double-reciprocal plots. For transient kinetics, the rate of NTP-induced dissociation of acto-HMM and the rate of NTP binding and cleavage were measured using a using a Hi-Tech PQ/SF stopped-flow sample handling unit (with a dead time of 2.1 ms) (Salisbury, England) interfaced with an OLIS Spectrofluorimeter, data acquisition unit, and software (OLIS, Silver Springs, GA). The rate of NTP binding to HMM was measured using exciting light at 295 nm (from a grating monochrometer with 1-mm slit width) from a 150-W xenon arc lamp, and the change in protein fluorescence at 90° to the incident light was monitored using a photomultiplier at wave lengths greater than 345 nm after passing through a WG 345 filter. The rate of acto-HMM dissociation was monitored by the change in light scattering at 365 nm (Johnson and Taylor, 1978; White et al., 1993). Estimates of the equilibrium constant for NTP cleavage were made using a single-turnover/cold chase technique (Bagshaw and Trentham, 1973). In these experiments, a 10-fold excess of HMM S-1 was mixed with [γ-^{32}P] NTP or [^{3}H] NTP and, after the nucleotide bound to and equilibrated with the HMM (as judged from the increase in protein fluorescence), 2 mM unlabeled NTP was added. Aliquots of the reaction solution were quenched in 1 N H_3PO_4, mixed, allowed to stand on ice for 5 min, and then brought to pH 4.6 with 1 N NH_4OH. Carrier NTP, NDP, and NMP were added to the solution, which was centrifuged in an Eppendorf tabletop centrifuge for 5 min. Aliquots of the supernatant were injected onto a SAX analytical column (see above), and the isocratically eluted NTP and NDP peaks were collected and analyzed by scintillation counting to determine the extent of NTP hydrolysis. Experiments were conducted under conditions similar to those for fibers (10°C, pH 7.1, 200 mM ionic strength) and the in vitro motility assay (25°C, pH 7.4, 54 mM ionic strength). The protein solutions at 10°C contained 100 mM BES (pH 7.1), 2 mM K_2EGTA, 1 mM free Mg^{2+}, 1 mM DTT, and 163 mM K-acetate, and those at 25°C contained 25 mM KCl, 25 mM MOPS (pH 7.4), 2 mM K_2EGTA, 2 mM $MgCl_2$, and 1 mM DTT).

RESULTS

Survey of NTPs

The isometric force (P_o), stiffness (S_o), and V_u produced by fibers with 6 mM ATP were compared with the force (P_{NTP}), stiffness (S_{NTP}), and unloaded shortening velocity ($V_{u[NTP]}$) produced in the same fiber when ATP was replaced with 6 mM NTP. Comparisons for the survey of NTPs were made at 6 mM nucleotide concentration to insure that V_u was at maximum for ATP (Cooke and Bialek, 1979). The results of this survey are summarized in Table 1. The level of P_{NTP} occurred in the following order: ATP = dATP > CTP = dCTP > UTP = dUTP > GTP > ITP. P_{CTP} and P_{dCTP} were only slightly reduced from P_o, whereas P_{UTP} and P_{dUTP} were reduce by half, and P_{GTP} and P_{ITP} were <17% P_{ATP}. S_{NTP} was similar to P_{NTP} and had the relationship ATP = dATP = CTP = dCTP > UTP = dUTP > GTP > ITP. As a control, stiffness was measured under rigor conditions and was found to be 130 ± 2%

TABLE 1 Relative values of P_{NTP}, S_{NTP}, and $V_{u(NTP)}$, by NTP

NTP	P_{NTP}	S_{NTP}	$V_{u(NTP)}$
ATP	1	1	1
dATP	0.98 ± 0.07 (20)	0.99 ± 0.06 (8)	1.27 ± 0.02 (20)
CTP	0.86 ± 0.02 (28)	1.02 ± 0.06 (4)	0.52 ± 0.03 (16)
dCTP	0.92 ± 0.03 (22)	1.0 ± 0.03 (3)	0.47 ± 0.03 (15)
UTP	0.47 ± 0.03 (24)	0.65 ± 0.05 (10)	0.17 ± 0.01 (10)
dUTP	0.47 ± 0.03 (18)	0.72 ± 0.06 (6)	0.26 ± 0.03 (10)
ITP	0.11 ± 0.01 (10)	0.29 ± 0.03 (3)	0.07 ± 0.01 (2)
GTP	0.17 ± 0.03 (7)	0.46 ± 0.02 (5)	0.04 ± 0.01 (5)

Values are mean ±SE (number of observations) expressed as a percentage of P_o (136 ± 5 S_o (12.4 kN/m^2), and V_u (1.8 ± 0.1 ML/s) in the same fiber. [NTP] = 6 mM for all observations.

(mean ± SE, $n = 23$) of S_o, in agreement with earlier data (Goldman and Simmons, 1984; Pate et al., 1993). Because S_{NTP} was compared to S_o in the same fiber (at the same sarcomere spacing), the ratio S_{NTP}/S_o should be roughly proportional to the number of strongly bound cross-bridges during isometric contractions (Ford et al., 1977). Measurements of the S_{NTP}/S_o ratio suggest that the number of strongly bound cross-bridges does not change for dATP, CTP, or dCTP, but was reduced for the other NTPs. For these NTPs (UTP, dUTP, ITP, and GTP), S_{NTP} was not reduced as much as P_{NTP} (Table 1). Similar stiffness-force relationships were reported by Pate et al. (1993) for CTP and GTP. The larger decrease in force (relative to stiffness) is similar to that seen when force is reduced by increasing P_i (Dantzig et al., 1992; Martyn and Gordon, 1992; Hibberd et al., 1985) or the addition of butanedione monoxime (BDM) (Regnier et al., 1995; Higuchi and Takemori, 1989), vanadate (Chase et al., 1993), aluminofluoride (Chase et al., 1993, 1994), or beryllofluoride (Regnier et al., 1997). Assuming that the compliance of the thick and thin filaments is unchanged in different nucleotides, the change may be produced by variation in the population of strongly bound, low-force-exerting cross-bridges (Regnier et al., 1995). Alternatively, these NTPs may alter the power stroke in a manner that reduces the force per cross-bridge in isometric contractions.

V_u varied widely for the various NTPs. Fig. 1 *a* shows typical slack test force traces after a 7% length step using ATP, dATP, CTP, and UTP in the same fiber. The "slack time," the time from the beginning of the length step to the point when force starts to redevelop, increases with the order dATP < ATP < CTP < UTP. Least-squares linear regression fits of the slack times for four length steps (ranging from 5% to 10% of fiber length) used to determine $V_{u[NTP]}$ are shown in Fig. 1 *b*. $V_{u[NTP]}$ for this fiber increased with the same order as shown for the single traces in Fig. 1 *a*. The $V_{u[NTP)}$ data for all of the NTPs surveyed are summarized in Table 1 and yield the relationship dATP > ATP > dCTP = CTP > dUTP > UTP > ITP > GTP. The results obtained for CTP and GTP agree with those of Pate et al. (1993). dATP was unique because P_{dATP} was similar to P_o, but $V_{u(dATP)}$ was greater than V_u by almost 30%. CTP and dCTP reduce isometric force only slightly, but reduce V_u by ~50%, whereas UTP and dUTP reduce force by ~50% and are poor substrates for fiber shortening. ITP and GTP are poor substrates for both force and shortening and were not studied further. dATP, CTP, and UTP were selected for further study because they support significant force and span a wide range of shortening velocities.

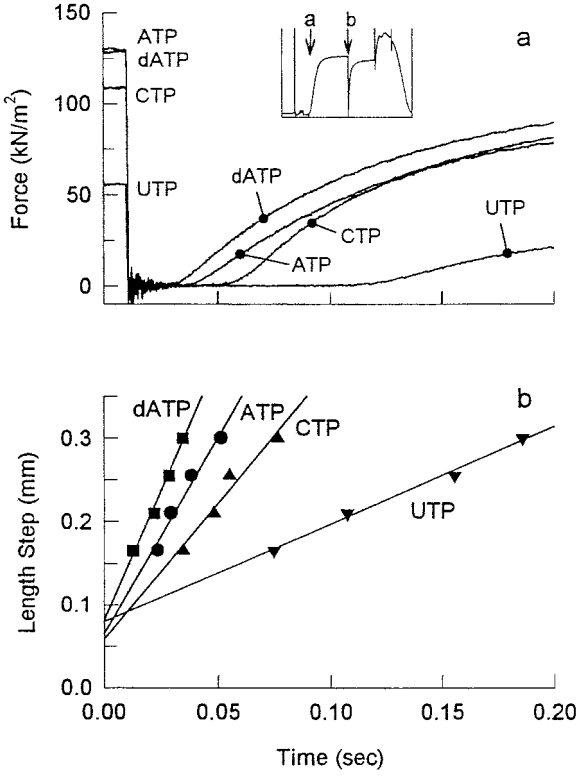

FIGURE 1 Isometric force ($P_{NTP)}$) and unloaded shortening velocity ($V_{u(NTP)}$) for ATP, dATP, CTP, and UTP in the same fiber. (*a*) The inset demonstrates the procedure used for measurements. At arrow a, the fiber was transferred from a preactivating solution (see Materials and Methods) to an activation solution containing 6 mM NTP (pCa 4.5), and force was allowed to develop to a steady-state condition. At arrow b, the fiber was unloaded by a quick release (of 7%), and force was allowed to redevelop at the shorter length before the fiber was transferred to relaxing solution. For this fiber, P_o = 133 kN/m², CSA = 3156 μm², and fiber length (at a sarcomere length of 2.8 μm) was 3.0 mm. Normalized force values are 1.0 (ATP), 1.0 (dATP), 0.85 (CTP), and 0.45 (UTP). (*b*) Plot of slack time versus length steps (5.5%, 7.0%, 8.5%, and 10% of fiber length) used to determine $V_{u(NTP)}$. The adjusted $V_{u(ATP)}$ for this fiber was 1.8 muscle lengths/s, and normalized values are 1.0 (ATP), 1.25 (dATP), 0.70 (CTP), and 0.27 (UTP).

Concentration dependence of P_{NTP} and $V_{u(NTP)}$ in fibers and $V_{f(NTP)}$ in motility assays

To determine the extent to which differences in fiber contractile properties with NTPs at 6 mM were associated with differences in NTP binding, we measured force and V_u at different NTP concentrations. In agreement with Cooke and Bialek (1989) and Ferenczi et al. (1984), P_o decreased linearly with log [ATP] for concentrations ranging from 0.1 mM to 5 mM (Fig. 2). This inverse correlation between substrate concentration and force was observed for all of the NTPs examined as well (Fig. 2). Over the concentration ranges used for these experiments, the slope of the force/log (NTP) for dATP, CTP, and UTP was not significantly different from that seen in ATP, which suggests that the equilibrium binding constants of the nucleotides to rigor cross-bridge state are similar.

As previously demonstrated for ATP (Cooke and Bialek, 1979; Ferenczi et al., 1984), the V_u of fibers increased with increasing [NTP]. Double-reciprocal plots of $1/V_{u(NTP)}$ versus 1/[NTP] are shown for ATP and dATP in Fig. 3 *a*, and for CTP and UTP in Fig. 3 *b*. The values for V_u are expressed relative to V_u with 6 mM ATP (1.0) in each fiber

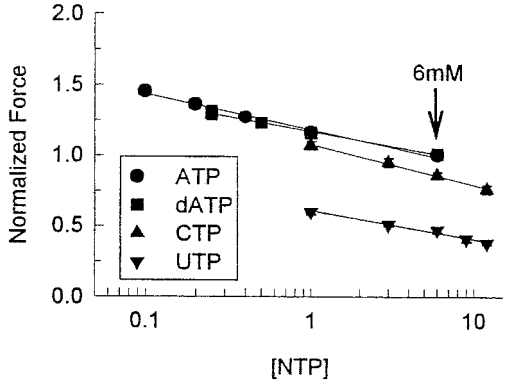

FIGURE 2 Concentration dependence of isometric force for ATP, dATP, CTP, and UTP. Values are normalized to the isometric force level at 6 mM ATP in the same fiber. Regression analysis (*solid line*) showed that force decreases linearly with log [NTP] for all of the nucleotides, over the ranges used for these experiments ($r^2 > 0.98$; n = 3–7 fibers for each NTP). Most SE bars are within the symbols.

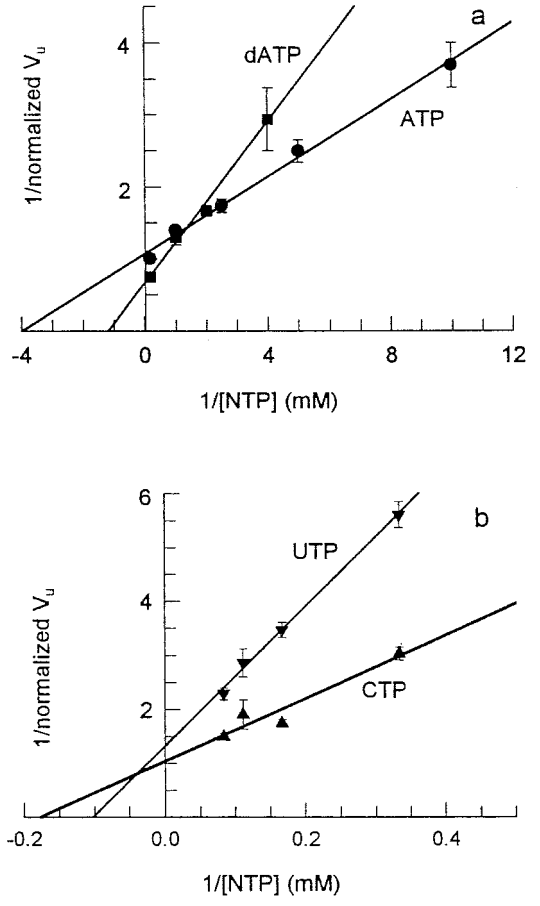

FIGURE 3 Double reciprocal plots of $1/V_u$ versus 1/[substrate] for (*a*) ATP (●) and dATP (■) and (*b*) CTP (▲) and UTP (▼). Values are the means ± SE for 3–7 fibers. The solid lines are least-squares linear fits (r^2 = 0.98) used to determine values for maximum $V_{u(NTP)}$ and the K_{app} (mM NTP) for half-maximum $V_{u(NTP)}$, summarized in Table 2.

for ease of comparison. The data for the four nucleotides obey Michaelis-Menten saturation behavior, allowing estimates of max V_u (V_u at infinite [NTP]) and K_{app}, shown in Table 2. The K_{app} for ATP was within the range of published values and was about threefold less than the K_{app} for dATP, but both were in the submillimolar range. Thus V_u is near maximum for both substrates at a concentration of 6 mM, and max V_u was 31% faster for dATP. K_{app} values for CTP and UTP were in the millimolar range, ≥20 times greater than for ATP. The large K_{app} values limit the NTP concentrations used for extrapolations to maximum V_u to the ascending (steep) limb of the substrate saturation curve. Nevertheless, the data suggest that UTP is a moderately good substrate for V_u (76% of ATP V_u), and CTP could produce shortening velocities similar to those in ATP if the [MgCTP] could be raised to 15 mM. The K_{app} may also be inflated by a the build up of NDP in the center of the fiber.

Elevated levels of ADP are known to reduce V_u in skinned muscle fibers (Cooke and Pate, 1989), and elevated CDP or UDP may also influence measurements of max V_u. HPLC analysis of activation solutions showed that contaminating levels of NDP were 1–3%, but because CDP and UDP are poor substrates for CPK (see above), these products may accumulate in the fiber contractile lattice. Therefore, an independent measure of the [NTP] dependence of shortening velocity was obtained by studying F-actin sliding speed or motility (V_f) in an in vitro motility assay (pH 7.4, 25°C) (Fig. 3, *a* and *b*). This method minimizes the problems associated with NDP accumulation, because the low concentration of contractile proteins in the motility assay preclude a significant rise in NDP (Harada et al., 1990). Measurements of V_f at [MgNTP] up to 5 mM (at least 3× K_{app}) gave results qualitatively similar to those found in fibers (Table 2). K_{app} was the same for ATP and dATP, resulting in an increased V_f with dATP at each substrate concentration and an increase in max V_f by 40%. The relatively higher K_{app} for CTP and UTP limits V_f at low substrate concentrations, but, as in fibers, maximum velocity in CTP was about the same as in ATP, and in UTP was 70% as fast as ATP. The qualitatively similar K_{app} and velocity results support the hypothesis that UTP and especially CTP are effective substrates for shortening at saturating substrate concentrations, and that dATP is more effective than ATP in shortening muscle fibers.

The differences in mechanical measurements with NTPs cannot be interpreted without additional information about

TABLE 2 [NTP] dependence of $V_{u(NTP)}$ for muscle fibers and F-actin motility

	Muscle fibers (10°C)		F-actin motility (25°C)	
NTP	K_{app} (mM)	max V_u (NTP/ATP)	K_{app} (mM)	max V_f (μm/s)
ATP	0.25	1	0.13	6.4 ± 0.6
dATP	0.76	1.31 ± 0.06	0.13	8.3 ± 0.4
CTP	5.62	1.01 ± 0.05	1.58	6.9 ± 0.7
UTP	9.83	0.76 ± 0.04	0.92	4.5 ± 1.3

Values for max V_u and max V_f are means ± SE.

various steps of the reaction mechanism. These include the actin-activated steady-state NTPase rate, the rate of NTP binding to the actomyosin cross-bridge and the subsequent rate of actomyosin dissociation, and the rate of NTP cleavage and the equilibrium constant for that cleavage. Below we report estimates of these rate constants, assuming that the basic mechanism of NTP hydrolysis is similar to that for ATP (Scheme 1).

Steady-state rate of hydrolysis of NTPs by HMM and acto-HMM

To examine the relationship between shortening velocity and the rate of substrate utilization, the steady-state hydrolysis rate of NTPs by HMM alone (V_{HMM}) and actin-activated HMM (V_{max}) was measured under low ionic strength conditions at 10°C and 25°C. At both temperatures V_{HMM} increased in the order CTP < ATP < dATP < UTP (Table 3). Taking V_{HMM} for ATP as 100% at 10°C, the rate was 134% for dATP, 68% for CTP, and >400% faster for UTP, with all of the differences being significant ($p < 0.05$). The large increase in V_{HMM} for UTP has been reported by others (Keilley et al., 1956; Weber, 1969), but the decrease for CTP is different from that reported by White et al. (1993), who found no significant difference from ATP. Because the steady-state rate is limited by the dissociation of P_i from the M·ADP·P_i state, V_{HMM} represents a lower limit for that transition. Measurements of V_{HMM} at 25°C revealed faster rates with relationships similar to those at 10°C (Table 3), indicating that the overall reaction mechanism has similar temperature sensitivities.

The rate of NTP hydrolysis by HMM was increased by actin and, as seen in Fig. 4, exhibited hyperbolic behavior with the actin concentration. The rate of NTP hydrolysis displayed saturation kinetics for all NTPs at high actin concentrations, allowing estimates of K_m and V_{max} from double-reciprocal plots (Table 3). At both temperatures, V_{max} increased by >100 fold over V_{HMM} for ATP, dATP, and CTP, but by <20 fold for UTP. K_m was the same for ATP and dATP, ~25% lower for CTP, and >10-fold lower for UTP at 10°C. Increasing the reaction temperature to 25°C increased V_{max} by about eightfold (from 10°C values) for ATP, CTP, and UTP and 12-fold for dATP, whereas the K_m for actin was increased by two- to fourfold for ATP and dATP, and seven to eightfold for CTP and UTP. Notable is the increased V_{max} for dATP compared to that of ATP, which is in qualitative agreement with the data of Shimizu et al. (1991). At 10°C the acto-HMM CTPase rate is ~10% less than the ATPase rate. White et al. (1993) have reported that the acto-S1 CTPase rate was ~30% greater than that for acto-S1 ATPase. This discrepancy may be related to our use of HMM as opposed to S1 by White et al.

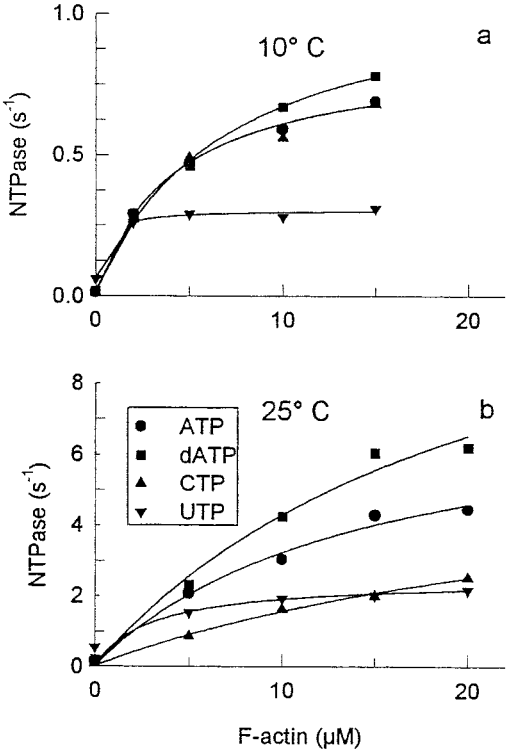

FIGURE 4 F-actin concentration dependence of acto-HMM NTPase for ATP (●), dATP (■), CTP (▲), and UTP (▼) at (*a*) 10°C and (*b*) 25°C. Reaction conditions at 10°C were the same as for fiber experiments, and at 25°C were the same as for in vitro motility assays, as reported in Materials and Methods. The data are fit (*solid lines*) to the equation $y = V_{max}([A]/([A] + K_m)$. Values for V_{max} and K_m were derived using double-reciprocal plots of the data, as in Fig. 3; the data are summarized in Table 3.

TABLE 3 Steady-state NTPase rate of HMM in the absence and presence of F-actin

NTP	HMM alone V_{HMM} (s^{-1})	Actin-activated V_{max} (s^{-1})	Actin-activated K_m (μm)
10°C			
ATP	0.0135 ± 0.0002	0.92 ± 0.06	5.4 ± 0.9
dATP	0.0181 ± 0.0006	1.01 ± 0.05	5.2 ± 0.7
CTP	0.0093 ± 0.0002	0.84 ± 0.07	4.0 ± 1.0
UTP	0.061 ± 0.007	0.31 ± 0.01	0.4 ± 0.18
25°C			
ATP	0.03 ± 0.0005	7.8 ± 1.5	14.4 ± 5.4
dATP	0.04 ± 0.0007	12.8 ± 1.9	21.5 ± 5.3
CTP	0.02 ± 0.0005	6.9 ± 1.2	29.6 ± 8.4
UTP	0.14 ± 0.004	2.5 ± 0.1	3.0 ± 0.4

The K_m for actin-activated NTPase is the apparent [NTP] that produces half-V_{max}.

The V_{max} for each NTPase rate correlates with $V_{u(NTP)}$ at 10°C and $V_{f(NTP)}$ at 25°C. It is notable that the dATPase rate is greater than that for ATP at both temperatures in the absence and presence of actin. This increase is similar in magnitude to the increased $V_{u(dATP)}$ and $V_{f(dATP)}$ (Table 2). In contrast, $V_{u(UTP)}$ and $V_{f(UTP)}$ correlate with V_{max} for UTP (relative to ATP), but are inversely related to V_{HMM}, suggesting that either the affinity of UTP for cross-bridges and/or the rate of UTP cleavage differs from ATP.

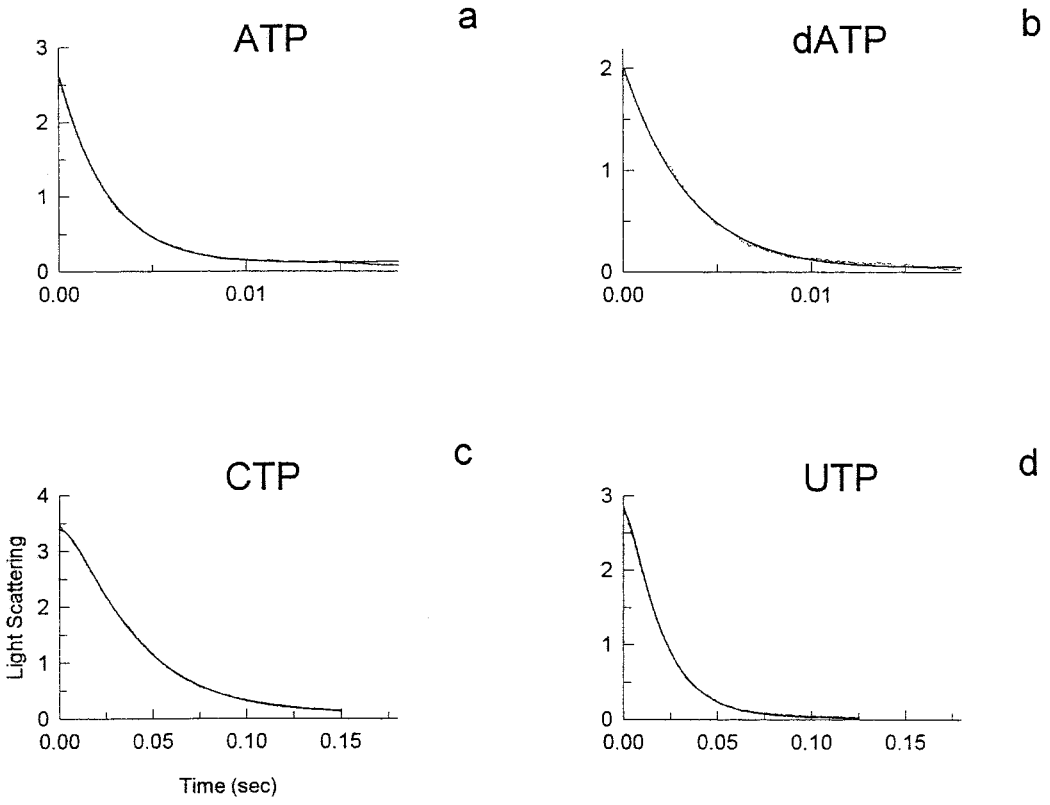

FIGURE 5 Time course of the decrease in light scattering by acto-HMM at a final concentration of 300 μM NTP. Conditions were the same as for fibers (i.e., 10°C, 0.2 M). The declines in light scattering in ATP and dATP were well fit by a single exponential, using the equation $y = A + B \cdot \exp(-\lambda t) + C \cdot t$ for (*a*) ATP and (*b*) dATP. The fits for these data (*solid lines*) yielded rates of 375 s^{-1} for ATP and 280 s^{-1} for dATP. The rate of decrease in light scattering was greatly reduced with (*c*) CTP and (*d*) UTP (note the 10-fold slower time scale) and had a lag phase. The data were fit as a two-step process ($A \rightarrow B \rightarrow C$) with a time course $P_1 + P_5 \cdot t + P_2[1 + (P_4 - P_3) \cdot (P_4 e^{(-P3 \cdot t)} - P_3 e^{(-P4 \cdot t)})]$, where P_3 is the time course of the lag phase, P_4 corresponds to the rate of decline of light scattering (i.e., the rate of formation of C) measured for ATP and dATP, P_1 is the starting point, P_2 is the amplitude change of light scattering, and P_5 is the linear slope of the data. For CTP (*c*), $P_3 = 124\ s^{-1}$, $P_4 = 25.8\ s^{-1}$; and for UTP (*d*), $P_3 = 232\ s^{-1}$, $P_4 = 57\ s^{-1}$. Axis labels are the same for each plot, as described in *c*.

NTP effects on the kinetics of acto-HMM dissociation

A more direct estimate of NTP affinity for cross-bridges was obtained by measuring the NTP-dependent rate of acto-HMM dissociation in a stopped-flow apparatus (see Materials and Methods). Fig. 5 shows the decrease in light scattering upon mixing of ~800 μM ATP, dATP, CTP, or UTP with acto-HMM at 10°C and 200 mM ionic strength. This change in light scattering monitors the dissociation of actin and HMM (White and Taylor, 1976). At this [NTP], the rate of acto-HMM dissociation increased with the order CTP < UTP < dATP ≤ ATP. The rates for dATP and ATP are not different. Fig. 6 shows the results of similar studies over a range of NTP concentrations from 50 μM to 1.6 mM. The data are fit to a hyperbolic relationship (see legend to Fig. 6), which yields the apparent second-order binding constants of the NTPs to acto-HMM (K_1k_a, Scheme 2) and the rate of actin dissociation from AM · NTP (k_a, Scheme 2) according to the following scheme:

$$\mathrm{AM + NTP} \overset{K_1}{\leftrightarrow} \mathrm{AM \cdot NTP} \overset{k_a}{\leftrightarrow} \mathrm{A + M \cdot NTP}$$

Scheme 2

where K_1 corresponds to the equilibrium constant for step 1 in Scheme 1 and k_a to the forward rate in step 2 of Scheme 1. The equations describing the kinetics of this reaction mechanism have been described by White (1982) and

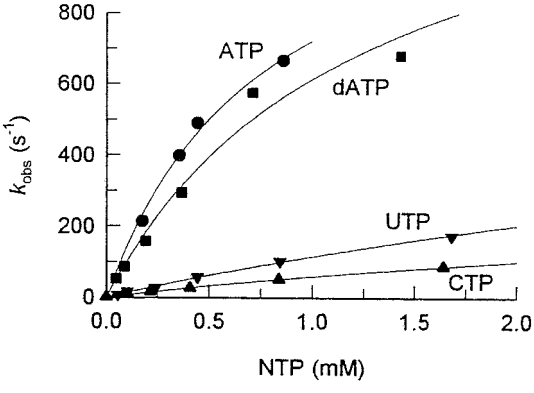

FIGURE 6 Rate of acto-HMM dissociation versus [NTP]. Lines are fits to the equation $k_{obs} = k_a/(1 + K_o/[NTP])$ and correspond to the reaction mechanism in Scheme 2. The results of these fits are summarized in Table 4.

Woledge et al. (1985). The experimental results are summarized in Table 4. They show that the apparent second-order rates of CTP and UTP binding are 10- to 20-fold less than those for ATP and dATP, and the smaller (K_1k_a) is predicted by the lower ratios of V_u/K_{app} and V_f/K_{app} obtained from the data in Table 2. Furthermore, the maximum rate of acto-HMM dissociation, k_a, in CTP was 350 s^{-1}, whereas values of ~1300 s^{-1} were obtained for ATP and dATP. The data indicate that each of these NTPs is effective in dissociating actin and myosin; consequently dissociation is unlikely to be rate limiting for steady-state NTP hydrolysis (except, perhaps, at low substrate concentrations). On the other hand, dissociation of actomyosin is relatively slow for CTP (190 s^{-1}) and UTP (360 s^{-1}) at 6 mM, a substrate concentration that produces the maximum V_u for ATP (1×10^3 s^{-1} rate of dissociation), and may therefore limit shortening velocity for these NTPs at this substrate concentration. The values of k_a for ATP and CTP obtained in these studies is about half those observed by White et al. (1993), although the K_1 values are about the same. The values obtained here may be underestimates in that the rates were measured to only the dissociation constant of CTP.

Estimation of the rate of NTP cleavage

The rate of NTP cleavage was measured using stopped-flow HMM protein fluorescence. Johnson and Taylor (1978) have shown that the time course of the protein fluorescence increase on binding ATP is the same as the time course of ATP cleavage as measured by quenched-flow techniques. Therefore we have assumed that the time course of the fluorescence change after mixing of HMM with NTP can be taken as a probe for the rate of NTP cleavage ($k_{+2} + k_{-2}$) according to Scheme 3:

$$M + NTP \underset{k_{-1}}{\overset{k_{+1}}{\leftrightarrow}} M \cdot NTP \underset{k_{-2}}{\overset{k_{+2}}{\leftrightarrow}} M \cdot NDP \cdot P \overset{k_{+3}}{\leftrightarrow} M + ADP + P_i$$

Scheme 3

Measurements were made at both 10°C, 200 mM ionic strength (pH 7.1), and 25°C, 50 mM ionic strength (pH 7.4) for comparison with fiber mechanics and F-actin motility data, respectively. Typical fluorescence increases after mixing of 1 mM NTP (producing a final NTP concentration of 500 μM) with 2 μM HMM (to produce a final HMM S-1 head concentration of 2 μM) are shown in Fig. 7. The solid lines are exponential fits to the protein fluorescence changes. At low substrate concentrations (15–250 μM), the average percentage increases in protein fluorescence produced by ATP, dATP, and CTP were, respectively, 10.88%, 11.87%, and 12.16%. As the substrate concentration was raised, the ATP and dATP amplitude did not decrease significantly (the stopped flow dead time was ~2.1 ms), but the rate of the fluorescence increase rose. The absolute protein fluorescence in CTP and UTP decreased with increases in nucleotide concentration, because these NTPs absorb significant amounts of exciting light at 295 nm. The similar amplitude of the percentage fluorescence increase for ATP, dATP, and CTP, however, suggests that the equilibrium constant for the cleavage step is similar.

The recording of the fluorescence change after the addition of UTP (seen in Fig. 7 *b*) gave a different pattern. UTP addition produces an initial fall in protein fluorescence, followed by a rise. When the traces at different UTP con-

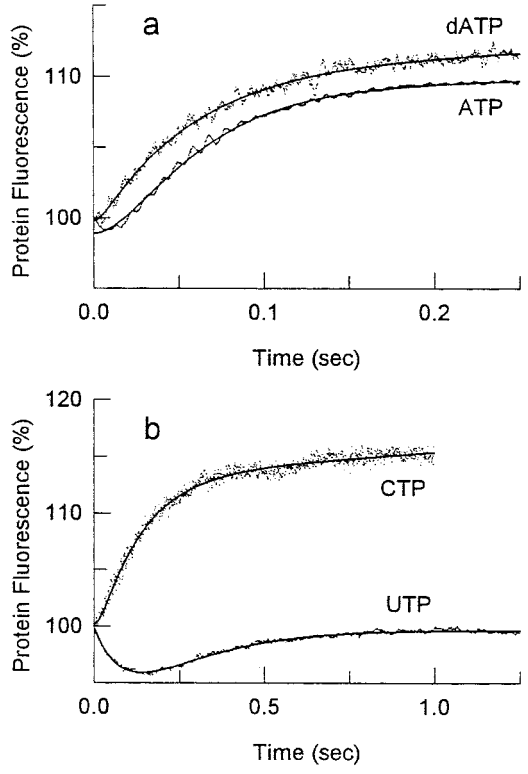

FIGURE 7 The time course of the increase in intrinsic fluorescence of HMM at a final concentration of 500 μM NTP (10°C). The reaction conditions are given in the Results. The data for ATP (*a*), dATP (*a*), and CTP (*b*) were fit (*solid lines*) using the lag equation described for Fig. 5, *c* and *d*. For ATP the rate constant for the lag fit was 38 s^{-1}, and the rate of protein fluorescence increase was 24 s^{-1}. Corresponding fits for dATP are 254 s^{-1} and 17 s^{-1}, whereas those for CTP are 48 s^{-1} and 8 s^{-1}. The trace for UTP(b) is fit with a double exponential ($y = A + B \cdot \exp^{(-\lambda 1 t)} + C \cdot \exp^{(-\lambda 2 t)}$), with a rate of fluorescence decrease of 10.7 s^{-1} (13.1 ± 1.6 s^{-1}, mean ± SEM, $n = 11$ for studies at 10°C) and a rate of fluorescence increase of 4.5 s^{-1}. This behavior is approximated by the equation

$$M^* \rightleftarrows M + UTP \rightleftarrows M\text{-}UTP \rightleftarrows M^{**}\text{-}UDP\text{-}P_i$$

where the relative fluorescence for M* = 1, M and M-UTP = 0.8, and M** · UDP · P_i = 1.05. The forward rate constant for protein isomerization is 15 s^{-1}, and the backward rate constant is 75 s^{-1}.

TABLE 4 The rate of acto-HMM dissociation by NTP at 10°C

NTP	K_1 (M^{-1})	k_a (s^{-1})	K_1k_a (M^{-1} s^{-1})
ATP	1.24×10^3	1290 ± 170	1.6×10^6
dATP	7.9×10^2	1386 ± 103	1.1×10^6
CTP	2.0×10^2	354 ± 54	7.0×10^4
UTP	1.5×10^2	870 ± 37	1.3×10^5

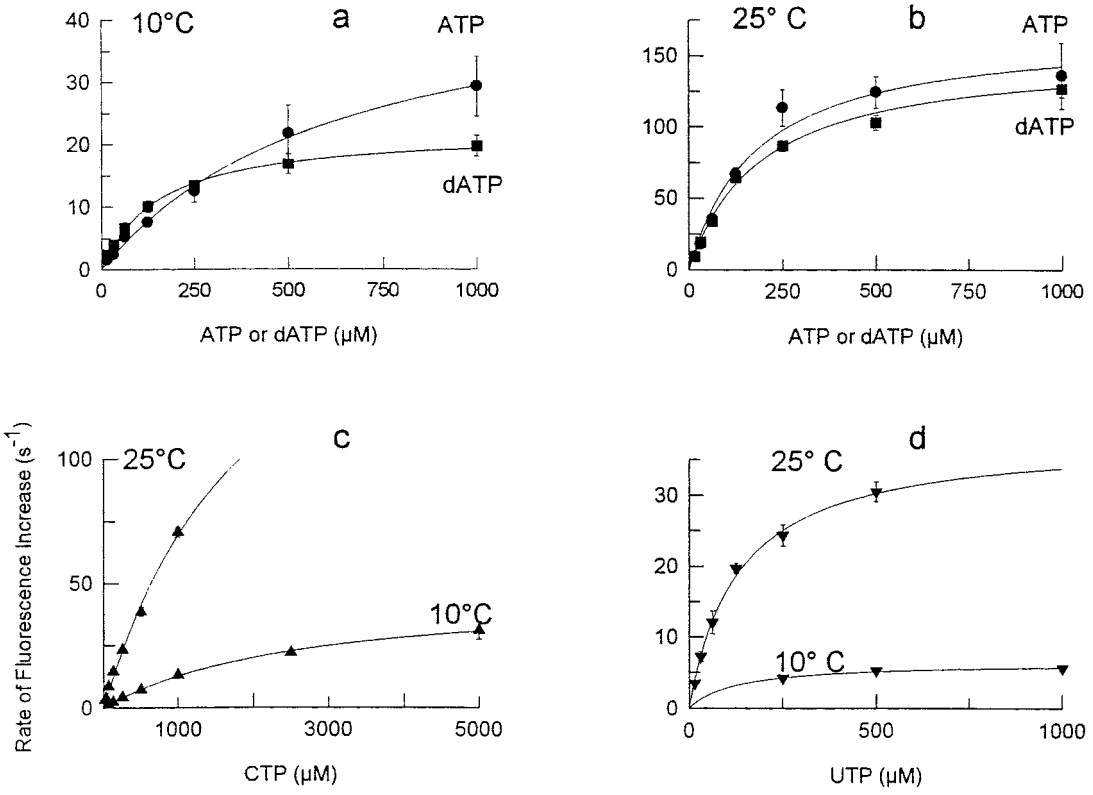

FIGURE 8 Rate of the increase in intrinsic fluorescence of HMM upon the addition of NTP versus [NTP]. Hyperbolic fits to the data (*solid lines*) were used to determine $k_{+2} + k_{-2}$ (Scheme 3) and K_m, which are summarized in Table 5. At 10°C, 0.2 M ionic strength, the apparent second-order rate constants were (in M^{-1} s^{-1}) as follows: ●, ATP = 8.0×10^4 (*a*); ■, dATP = 9.0×10^4 (*a*); ▲, CTP = 1.4×10^4 (*c*); and at 25°C, 55 mM ionic strength: ATP = 5.6×10^5 (*b*), dATP = 5.1×10^5 (*b*), CTP = 2.0×10^5 (*c*); ▼, UTP = 1.7×10^5 (*d*).

centrations were fitted by a double exponential, we found that the absolute amplitude of initial decrease in protein fluorescence averaged 0.62 ± 0.03 of the subsequent fluorescence rise and did not change with [UTP]. The rate of the fluorescence decrease averaged 56 ± 6 s^{-1} (mean ± SEM, $n = 31$) and did not change significantly with [UTP] at 25°C. However, the rate of the subsequent fluorescence increase rose hyperbolically with [UTP] (see Fig. 8). The simplest model approximating these changes is the following. We assumed that the HMM exists in two forms: a higher fluroescent form (M*), which does not bind UTP significantly, and a second isomer (M, having a lower fluorescence), which can bind UTP and produces no fluorescence change. (We further assume that ATP, dATP, and CTP can bind to both M* and M.) The hydrolysis forming M** · UDP · P_i then increases the protein fluorescence, as with the other nucleotides. The rate of fluorescence decrease on UTP addition is produced by the kinetics of the equilibrium between the two nucleotide-free HMM isomers. Further details are given in the legend to Fig. 7.

The rates of the fluorescence increases in Fig. 7 are 24.2 s^{-1} for ATP, 17.4 s^{-1} for dATP, 7.8 s^{-1} for CTP, and 4.5 s^{-1} for UTP. Fig. 8 shows plots of the rates of the fluorescence increases as a function of nucleotide concentrations at 10°C and 25°C, and hyperbolic fits to the data (shown as *lines*) are summarized in Table 5. The most significant finding here is the similarity of $(k_{+2} + k_{-2})$ for ATP, dATP, and CTP at both 10°C and 25°C. The rate for UTP is, however, only 12–25% as fast. The similarity of behavior for ATP and dATP and the relatively high rates (compared to NTPase rates) render it unlikely that the cleavage rate produces the differences in V_u for these two nucleotides. Similarly, even though the apparent K_m for CTP is high, the

TABLE 5 Rate of HMM fluorescence increase on NTP binding

NTP	$k_{+2} + k_{-2}$ (s^{-1})	K_m (mM)
10°C		
ATP	49 ± 3	0.7 ± 0.08
dATP	23 ± 1	0.2 ± 0.01
CTP	47 ± 2	2.7 ± 0.20
UTP	6 ± 0.2	0.13 ± 0.02
25°C		
ATP	168 ± 14	0.18 ± 0.04
dATP	152 ± 5	0.19 ± 0.02
CTP	219 ± 47	2.10 ± 0.60
UTP	38 ± 1	0.13 ± 0.01

Reaction conditions for 10°C were 200 mM ionic strength, 100 mM BES (pH 7.1), 2 mM $MgCl_2$, 1 mM DTT. Reactions conditions for 25°C were the same as for the in vitro motility assay (see Materials and Methods).

cleavage rate should be fast enough that it is not the limiting factor in $V_{u(CTP)}$ at 10°C with 6 mM CTP.

Measurement of the equilibrium constant for NTP cleavage (K_2)

For measurements of the cleavage equilibrium constant ($K_2 = k_{+2}/k_{-2}$, Scheme 3), the single-turnover and cold chase techniques of Bagshaw and Trentham (1973) were used. In these experiments [γ-^{32}P]NTP (final concentration 1 μM) was mixed with S-1 (as HMM; final S-1 head concentration 11 μM at 200 mM ionic strength, pH 7.1, 2 mM $MgCl_2$, 10°C) at time 0. Parallel studies of increased protein fluorescence with NTP binding under the same conditions showed that NTP binding was at maximum at 6 s for ATP and dATP and at 20 s for CTP (Fig. 9). It is assumed that most of the NTP is bound to S-1 and equilibrates between M · NTP and M · NDP · P_i (Scheme 3). The method further assumes that $k_{+2} + k_{-2}$ is rapid compared to k_{+3}, and this is approximately true, because the HMM k_{cat} (Table 3) and the rate of fluorescence decay after the fluorescence peak are 15–240 times slower than $k_{+2} + k_{-2}$. At the peak fluorescence increase (6 s for ATP and dATP and 20 s for CTP), 2 mM unlabeled NTP (cold chase) was added to the reaction mixture to prevent any [γ-^{32}P]NTP that dissociates from the S-1 from rebinding to the S-1. Aliquots of the solutions were taken and quenched, and the amounts of NTP and NDP were determined in the sample. The ratio of NDP/NTP immediately after the cold chase is the ratio of k_{+2}/k_{-2}. The results in Tables 6 and 7 also show that the NDP/NTP ratio (K_2) in ATP (1.42) and dATP (1.42) is the same (implying that K_2 is the same for both nucleotides). However, the NDP/NTP ratio in CTP is larger (13.5) than those from ATP and dATP. From these data the calculated values for K_2 at 10°C can be coupled with the stopped flow measures of cleavage rate ($k_{+2} + k_{-2}$, Scheme 3), allowing the estimations of k_{+2} and k_{-2} shown in Table 7.

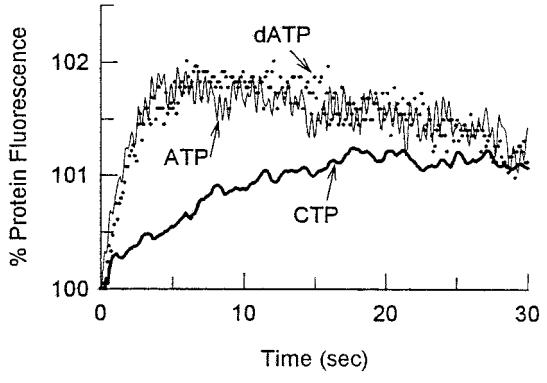

FIGURE 9 Time course of HMM fluorescence increase used to determine when NDP and NTP come into equilibrium for ATP (*thin solid line*), dATP (*dots*), and CTP (*thick solid line*). Conditions were as described in the Results for cold chase experiments. NTP cleavage equilibrium occurred at 6 s for ATP and dATP and at ~20 s for CTP.

TABLE 6 Single-turnover experiments

Substrate	Cold chase time (s)	Quench time (s)	NDP	NTP
ATP	6	10	0.59	0.41
dATP	6	10	0.59	0.41
CTP	20	30	0.93	0.07

Nucleotide values are fraction of total measured at given quench time.

TABLE 7 Estimation of HMM cleavage equilibrium and rate constants, for HMM at 10°C

NTP	K_2	k_{+2} (s^{-1})	k_{-2} (s^{-1})
ATP	1.42	29 ± 2	20 ± 1
dATP	1.42	14 ± 1	9 ± 1
CTP	13.5	42–44	3.0–5.0
UTP*	2.6	4.3 ± 0.1	1.7 ± 0.1

*K_2 estimated from zero-time intercept of UTP hydrolysis rate.

The method described above could not be used for measurements of K_2 with UTP, because the fluorescence signal used to indicate the point in time at which the NDP and NTP come into equilibrium (Fig. 9) was indistinguishable from background noise under single-turnover conditions. To obtain a rough estimate of K_2, HMM (final concentration was 21 μM S-1 heads) was mixed with [γ-^{32}P]UTP (100 μM final concentration). The reaction was quenched at 5, 20, 40, and 60 s, after the initiation of the reaction and the fraction of [γ-^{32}P]UTP hydrolyzed was measured. A regression of the percentage of [γ-^{32}P]UTP cleaved against time gave a zero time intercept of 15.1 μM [γ-^{32}P]UTP, or 0.72 of the S-1 heads present (Fig. 10). Assuming that all of the S-1 heads are active, this result implies a K_2 for UTP of 2.6 ($K_2 = 0.72/0.28$). This value, coupled with the low maximum cleavage rate (see above), suggests a much slower

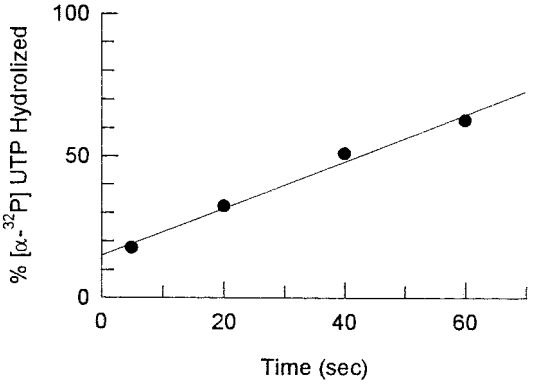

FIGURE 10 Time course of [γ-^{32}P] UTP hydrolysis by HMM used to estimate UTP P_i burst size. At zero time [γ-^{32}P]UTP was mixed with HMM (final concentration 100 μM [γ-^{32}P]UTP and 21 μM HMM S-1 heads), and the reaction was acid-quenched at 5, 20, 40, or 60 s. Linear fits to the data yield an intercept of 15.1 μM with a slope of 0.825 %/s. Thus the P_i burst size indicates that the ratio 15.1 FM/21 μM = 0.72, so that the ratio k_{+2}/k_{-2} (Scheme 3) is 0.72/0.28 or 2.6. The [γ-^{32}P]UTPase rate was 0.04 s^{-1}.

forward rate for UTP cleavage (k_{+2}) than for ATP, dATP, and CTP (Table 6).

DISCUSSION

The present study confirms earlier reports that most NTPs, when used as substrates for contractions, produce less isometric force and a slower shortening velocity than that for ATP at comparable nucleotide concentrations (Pate et al., 1991, 1993; White et al., 1993). However, the most interesting finding was that V_u is increased when dATP replaces ATP, whereas isometric force is unchanged. dATP is one of the few substrates that allows a faster shortening velocity in the muscle and motility assay than ATP, increasing both max V_u and max V_f by ~30%. Velocity was also faster for dATP at all submaximum nucleotide concentrations. This contrasts with the findings of Shimizu et al. (1991), who reported a slightly slower V_f (87% that of ATP) at 1 mM nucleotide. The difference may be a consequence of the lower ionic strengths used in their studies. At comparable ionic strengths, Shimizu et al. (1991) do report faster myosin S-1 dATPase rates in both the presence and absence of actin, in agreement with our measurements (Table 3).

Isometric force is significantly reduced in the presence of CTP and UTP, whereas maximum shortening velocity or sliding speed is similar for ATP and CTP, but is reduced in UTP. Measurement of V_u in fibers at 6 mM CTP implied that in CTP, V_u is reduced. However, experiments at increased MgNTP showed both in skinned fibers and in motility assays that this apparent reduction was a consequence of the relatively weak binding of MgCTP to actomyosin (Tables 2, 4, and 5). UTP, despite its greater K_1k_a for actomyosin dissociation (compared to CTP), supports a significantly reduced V_u. Muscle stiffness during isometric activation in ATP, dATP, and CTP is the same, whereas that in UTP is reduced. Although a significant fraction (~50%) of the isometric compliance occurs in the thick and thin filaments, these components are unlikely to change in different nucleotides. The decline in muscle stiffness in UTP may be a result of at least three factors: 1) the number of strongly bound cross-bridges (AM* · NDP · P_i, AM* · NDP, AM*) may be reduced; 2) the number of weakly bound cross-bridges (AM · NDP · P_i) may be increased at the expense of strongly bound cross-bridges; 3) or the numbers of both weakly and strongly bound cross-bridges may decline.

There is an intriguing proportionality between unloaded shortening velocity and actin-activated NTPase, which is most clearly seen in Tables 2 and 3. Regression of the relative V_u and relative V_f against the relative acto-HMM V_{max} is well fitted ($R^2 = 0.994$) by an equation in which

$$\text{rel } V_u(\text{rel } V_f) = 0.55 + 0.53*(\text{rel } V_{max})$$

However, unloaded shortening velocity does not correlate with NTP cleavage rates, cleavage equilibrium constants, or rate of acto-S1 dissociation. On what do filament sliding speed, force, stiffness, and isometric NTPase depend?

Determinants of force, shortening velocity, and stiffness

Insight into this question can be gained by systematically examining the change in force, shortening velocity, and isometric NTPase rates predicted by the strain-dependent Pate-Cooke cross-bridge model in Fig. 11. The Pate-Cooke cross-bridge model involves five steps: 1) NTP cleavage by myosin, M · NTP (state 1) to form M · NDP · P_i (state 2); 2) binding of the M · NDP · P_i to actin to form AM* · NDP · P_i (state 3), which exerts force (both positive and negative); 3) a power stroke in which P_i is released to produce force, movement, and AM* · NDP (state 4); 4) the release of NDP from AM* · NDP to form the AM* rigor linkage (state 5; this step does not produce additional force or shortening); 5) NTP binding to the rigor linkage and the subsequent dissociation of AM* to M · ATP and actin. The asterisk (*) near M designates strongly bound, force-exerting states. The model assumes a cross-bridge stiffness, a cross-bridge throw, free energy changes between the various states, forward (R_{ij}) and reverse (R_{ji}) rate constants between the *i*th and *j*th states, and most importantly, a strain dependence of the different cross-bridge states. The model successfully accounts for the force-velocity curve and the [ATP], [ADP], and [P_i] dependence of both force and unloaded shortening velocity. We programmed the model using Quickbasic, and have used Cooke and Pate's (1989) rate constants, free energy changes, and cross-bridge strain dependencies. We changed only the rate and equilibrium constant for ATP cleavage, given the results of the experiments above. The force exerted in the muscle, expressed as the sum of the forces exerted by all cross-bridges in the range from −12 to 12 nm, is then divided by the number of cross-bridges in this range to obtain an average force. The value is ~0.54 pN/cross-bridge and corresponds to ~2.16 pN/attached cross-bridge. The model V_u and isometric ATPase are almost identical to those reported by Cooke and Pate (1989). We next examined the sequelae of increases and decreases of each of the forward rate constants (by 2–10-fold) in their model on force, unloaded shortening velocity, stiffness, and isometric NTPase rate.

The model calculations show that changes in the rate constants that regulate the entry into or exit of cross-bridges from strongly bound states reduce force and stiffness, whereas changes in the rates of transitions that govern the transition of cross-bridges from negatively strained, strongly bound states strongly affect V_u. The results of those

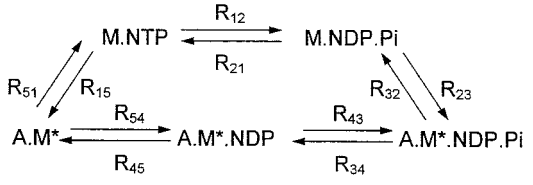

FIGURE 11 The Pate-Cooke cross-bridge model with associated forward (R_{12}, R_{23}, . . .) and reverse (R_{21}, R_{32}, . . .) rate constants.

TABLE 8 Change in force (P_o), unloaded shortening velocity (V_u), and Isometric ATPase rate with changes in various rate constants

Rate constant (% of control)	ΔP_o (% of control)	ΔV_u (% of control)	Δ isometric ATPase (% of control)
R_{12} (150%, K_{eq} = 10, CTP)	−6*	No change	3
R_{12} (14%, K_{eq} = 2, UTP)	−19	No change	−25
R_{12} (67%, K_{eq} = 1.5, dATP)	−2	No change	−3
R_{23} (200%)	6	2	33
R_{23} (50%)	−7	−2	−25
R_{34} (200%)	3	29	6
R_{34} (50%)	−1	−28	−5
R_{45} (150%)	−6	14	21
R_{45} (33%)	12	−42	−36
R_{51} (200%)	No change	10	1
R_{51} (10%)	No change	−54	−3
G_o (50%)	4	−40	−5
G_o (150%)	No change	No change	No change

For control, isometric force averages 2.16 pN/attached cross-bridge, unloaded shortening velocity is 1580 nm/hs/s, and isometric steady-state ATPase rate is 0.92 s^{-1}.

*The change in force is negative because the change in K_{eq} requires that $G_2(i) = 2.3RT$; because $G_3(i) = 4.3RT$ at its equilibrium point, the decrease in $G_2(i)$ necessitates that in the transition from M · NDP · P_i to AM · NDP · P_i, less energy is released and the force exerted by the AM · NDP · P_i state must be reduced.

simulations are summarized in Table 8, which indicates that 1) changes in the rates of the power stroke (step 3) and AM* dissociation (step 5) have little or no effect on the isometric force, but large effects on V_u; 2) changes in the NTP cleavage rate or equilibrium constant (step 1) or cross-bridge attachment (step 2) have significant effects on isometric force, but little effect on unloaded shortening velocity; 3) posthydrolysis attached state transitions (steps 3, 4, and 5) exert a strong influence on shortening velocity, but only the rate-limiting release of ADP has a signficant effect on force. The effect of changes in R_{51} on V_u are significant only if they apply to the rates at negative strain (i.e., at $x < 0$). The apparent second-order rate constant used for R_{51} (at $x < 0$) in the Pate and Cooke model assumes a linear increase in the rate with increases in ATP (10^4 s^{-1} at 6 mM ATP), whereas stopped flow measurements indicate that it saturates at 800-2200 s^{-1} (White et al., 1993; Ma and Taylor, 1994; this paper); 4) finally, the isometric ATPase rate is significantly affected by moderate changes in each step, except the rate of cross-bridge detachment by NTP binding (step 5). The effects of changing the free energy for NTP hydrolysis ($G0_o$) are also shown in Table 8. Using this model, the observed changes in rates measured in these experiments, and trial and error changes in the various rate constants given below, we obtained reasonable fits for the observed changes in isometric force, stiffness, and V_u by the alterations shown in Table 9. We next consider the changes and implications of each of the NTPs characterized.

ATP

The rate constants and strain dependency for ATP as a substrate were those used by Cooke and Pate (1989), aside from the fact that the free-energy change for the M · ATP to M · ADP · P_i step was reduced to $-0.4 * RT$, to take into account our measured value for the cleavage step (step 2), and the forward rate constant for cleavage was set to 30 s^{-1}, based on our measurements (Tables 5–7). The value for R_{51} was set at K_1k_a[ATP]/(1 + K_1[ATP] for $x > 0$ from the data in Table 4, rather than the apparent second-order rate constant of 2×10^5 M^{-1} s^{-1} used by Cooke and Pate (1989). This is because the use of the second-order rate constant ignores the fact that k_a limits the rate of dissociation by ATP under zero strain to ~1300 s^{-1}. Furthermore, our measured rates of ATP-induced association are in reasonable agreement with similar measurements by Johnson and Taylor (1978), Ma and Taylor (1994), and White et al. (1993). For

TABLE 9 Comparison of Pate-Cooke model predictions and measured values

Substrate	Condition	Rel. P_o	Rel. stiffness	Rel. V_u
ATP	Model*	1	1	1
	Measured	1	1	1
dATP	Model	0.94	0.96	1.28
	Measured	0.98	0.99	1.27
CTP	Model	0.84	0.82	0.56
	Measured	0.86	1.02	0.52
UTP	Model	0.46	0.60	0.26
	Measured	0.47	0.65	0.17

For ATP, R_{12}/R_{21} = 30/20; R_{23}, R_{34}, R_{45} as in Pate and Cooke (1989); $R_{51} = 1.6 \times 10^6$[ATP]/(1 + 1240[ATP]) for $x = 0$ or >0; and $R_{51} = (1.6 \times 10^6$[ATP] $- 4 \times 10^4(x))$/(1 + 1240[ATP]) for $x < 0$.

For dATP, R_{12}/R_{21} = 20/14; increase both R_{34} and R_{45} by 30%; $R_{51} = 1.1 \times 10^6$[dATP]/(1 + 790[dATP]) for $x = 0$ or >0, and $R_{51} = (1.1 \times 10^6$[dATP] $- 4 \times 10^4$ $(x))$/(1 + 790[dATP]) for $x < 0$.

For CTP, R_{12}/R_{21} = 45/5; R_{23} reduced to 60%; R_{34} and R_{45} increased by 50%; $R_{51} = 7 \times 10^4$[CTP]/(1 + 200[CTP]) for $x = 0$ or >0, and $R_{51} = 7 \times 10^4$[CTP] $- 1200x$/(1 + 200[CTP]) for $x < 0$.

For UTP, R_{12}/R_{21} = 4/2; R_{23} reduced to 40%; R_{34} increased to 200%; R_{45} to 500%; and $R_{51} = 1.3 \times 10^5$[UTP]/(1 + 150[UTP]) for all values of x.

*Force is 2.01 pN/attached cross-bridge, fraction cross-bridges attached is 0.54, V_u is 1470 nm/hs/s, and isometric ATPase is 0.92 s^{-1}.

negative strains, at $x < 0$, it was necessary to make R_{51} dependent on cross-bridge strain, because using the values obtained from stopped flow studies resulted in a computed V_u of 400 nm/hs/s, ~1/4 the observed value. By letting $R_{51} = (K_1 k_a[\text{ATP}] - 4 \times 10^4 \cdot (x))/(1 + K_1[\text{ATP}])$ for $x < 0$, an isometric force, V_u, stiffness, and isometric ATPase rate practically identical to those in Table 8 were obtained. A similar strain dependency was used for every ATP analog, as detailed in Table 9.

dATP

The rate constants for dATP cleavage and actomyosin dissociation and the equilibrium constant for cleavage were not much different from those for ATP, and their inclusion in the Pate-Cooke model did not significantly change the force, V_u, or isometric dATPase. Because the rate-limiting step for the dATPase is subsequent to cross-bridge attachment and in the model is controlled by the release of NDP from AM* · dADP, we increased the rate of R_{45} to increase the dATPase and to increase V_u. Increasing R_{45} by 30% at all cross-bridge strains increases the isometric dATPase by only ~8%, V_u by 8%, and decreased isometric force by 7%. To better approximate the observed changes in mechanics, we next increased the rate entering the power stroke (R_{34}) by 30%, a change that brought the force, V_u, and dATPase rate close to observed values (see Table 9). These changes produce an increase in ATPase and V_u, but leave isometric force and stiffness essentially unchanged. R_{34} and R_{45} are rate constants for posthydrolysis steps that cannot be directly measured. However, increases in these steps should increase both k_{tr} and k_{Pi}. The behavior of posthydrolysis steps is considered in the following paper.

Using the changes in R_{34} and R_{45} above suggests that the power output in the presence of dATP will be ~12% greater than that in the presence of ATP. However, the dATPase will be ~12% greater as well, suggesting no real change in contractile efficiency. This, plus the fact that the binding of dATP to myosin, its cleavage, and its ability to dissociate actomyosin as well as ATP, indicates that the lack of an oxygen on the 2 position of the ribose ring does not limit its effectiveness as a substrate for myosin. dATP can substitute for ATP in a variety of enzymatic reactions that influence muscle fiber contractions, as judged by the rapid rephosphorylation of dADP by the CP/CPK reaction. This property ensures that mechanical and kinetic properties are not influenced by product build-up.

CTP

The equilibrium constant for CTP cleavage and the estimated forward rate constant for cleavage were put into the Pate-Cooke model. Next, R_{51} at all cross-bridge displacements was reduced to the values observed in AM dissociation experiments (Table 4), with a corresponding reduction in the strain dependency at $x < 0$ (see Table 4 and footnote of Table 9). These changes reduced V_u to 40%, isometric force to 94%, and raised the isometric CTPase rate to 104% of that in the muscle. To reduce both the force and CTPase rate, R_{23} was reduced to 60% of its value in ATP, which brought the isometric force to 89% and V_u to 40% of the corresponding values in ATP. Finally, both R_{34} and R_{45} were increased by 50% above their value in ATP, to raise V_u to 56% and isometric force to 84% of their values in ATP. These results are in reasonable agreement with the experimental changes, as seen in Table 9. The step(s) limiting fiber shortening in 6 mM CTP differs from those for ATP or dATP. Estimates of max V_u, max V_f, and actin-activated steady-state CTPase all suggest that if enough substrate could be made available, fiber shortening velocity would be similar to or greater than the values in ATP. Because the cleavage rate for CTP (at 10°C) is fast (Table 6), either CTP binding to AM or the subsequent dissociation of actin from the M · CTP cross-bridge are rate limiting at a substrate concentration of 6 mM. This means that the attached AM* and AM* · CTP cross-bridge states accumulate during contractions in CTP. An increase in either of these populations could explain why fiber stiffness in CTP is similar to that in ATP, whereas force is reduced by ~15% (Table 1). Furthermore, the drag force (negative strain) created by these cross-bridge states markedly reduces V_u. Increasing the CTP concentration in the model to 24 mM raises V_u to 84% of that in ATP. The somewhat greater stiffness measured than predicted by the model may be a consequence of an accumulation of CDP in the fiber lattice secondary to the low rate of CDP phosphorylation by CPK. The combined effects of an increase in R_{34} and a decrease in R_{23} suggest that both k_{tr} and k_{Pi} will be increased in the presence of CTP.

UTP

Reducing R_{12} to 4, the cleavage equilibrium constant to 2, and setting R_{51} to $(1.5 \times 10^5[\text{UTP}]/(1 + 150[\text{UTP}]))$ for all values of x, and doubling R_{34} (in accordance with data in the following paper, Regnier and Homsher, 1998) in the presence of UTP reduced the model isometric force to 82% and V_u to 28% of the corresponding values in ATP. To lower isometric force still further, R_{23} was reduced to 40% and R_{45} increased to 500% of their values in ATP, yielding an isometric force of 46%, a V_u of 27%, and a stiffness of 66% of those seen in ATP. The reduction in R_{23}, which implies that the S-1 and actin binding sites may not interact in the normal fashion, should reduce k_{tr}. Futhermore, the increased R_{34} and R_{45} will increase k_{Pi}.

Recently White et al. (1997) have shown that the rate of NTP cleavage by the attached cross-bridge (AM) is much slower than that of the dissociated cross-bridge (M) at low ionic strength. They suggested that during isometric contractions, the rate-limiting step of the cross-bridge cycle is the cleavage step by the AM-NTP cross-bridge. If this is so, the model employed above would need to be modified to

include the hydrolysis by the attached cross-bridge, by making the dissociation step in ATP binding strain dependent. Such a change would facilitate fitting of the data, because it would provide several additional parameters that can be varied in the modeling.

The variety of mechanical responses provided by NTPs must stem from differences in the structure of the nucleoside (and ribose) portions of the molecule. Pate et al. (1993) suggest that the mechanical response of fibers to CTP is more similar to ATP than GTP, because ATP and CTP share a close proximity of amino groups. When the structures of ATP and CTP are superimposed, the amino groups at the 4-position of CTP and the 6-position of ATP are in similar spatial locations, with a nitrogen-to-nitrogen distance of only 1.8 Å. This amino group, a hydrogen donor for hydrogen binding, has been suggested to play an important role in NTP hydrolysis (Pate et al., 1993). GTP, which has a carbonyl group at the 6-position and is a hydrogen acceptor for hydrogen bonding, is a very poor substrate for myosin or acto-HMM. UTP supports a greater force and velocity than GTP. This may be a consequence of the fact that the hydroxyl group at the 6-position in the purine ring is closer to being a hydrogen bond donor than a carbonyl group. Another and unexpected influence on V_u appears to be the 2-position on the ribose ring of the nucleotide, causing a significant increase in hydrolysis activity, V_u and V_f. The reasons for this are not clear, because the x-ray structure of the ADP · Al · F_4 · S1 by Fisher et al. (1995a,b) indicates that the ribose hydroxyl groups face toward the solution and do not interact with S-1 residues. It could be, however, that the removal of the 2-hydroxyl group causes a flattening of the ribose ring and weakens the dADP binding to the S-1 head. If so, this could increase the rate of dADP release from the attached cross-bridge and account for the increased rate of shortening in dATP.

The authors gratefully acknowledge the help of Dr. Larry Faller, of the Department of Medicine at UCLA, and Dr. James Sellers, of the National Institutes of Health, for allowing us the use of the stopped flow equipment in their laboratories. We also thank Payam Bostani, Bibiana Kim, Silvia Tejeda, and Alyona Bobkova for their excellent technical assistance.

This work was supported by Public Health Service Grant AR 30988 (EH).

REFERENCES

Bagshaw, C. R., and D. R. Trentham. 1973. The reversibility of adenosine triphosphate cleavage by myosin. *Biochem. J.* 133:323–328.

Bagshaw, C. R., and D. R. Trentham. 1975. Transient kinetic and isotopic tracer studies of the myosin adenosine triphosphatase reaction. *J. Supramol. Struct.* 3:315–322.

Cecchi, G., P. J. Griffiths, and S. Taylor. 1986. Stiffness and force in activated frog skeletal muscle fibers. *Biophys. J.* 49:437–451.

Chase, P. B., D. A. Martyn, and J. D. Hannon. 1994. Activation dependence and kinetics of force and stiffness inhibition by aluminofluoride, a slowly dissociating analogue of inorganic phosphate, in chemically skinned fibres from rabbit psoas muscle. *J. Muscle Res. Cell Motil.* 15:119–129.

Chase, P. B., D. A. Martyn, M. J. Kushmerick, and A. M. Gordon. 1993. Effects of inorganic phosphate analogues on stiffness and unloaded shortening of skinned muscle fibres from rabbit. *J. Physiol. (Lond.).* 460:231–246.

Cooke, R., and W. Bialek. 1979. Contraction of glycerinated muscle fibers as a function of the ATP concentration. *Biophys. J.* 28:241–258.

Cooke, R., and E. Pate. 1989. The effects of ADP and phosphate on the contraction of muscle fibers. *Biophys. J.* 48:789–798.

Dantzig, J. A., Y. E. Goldman, N. C. Millar, J. Lacktis, and E. Homsher. 1992. Reversal of the cross-bridge force-generating transition by photogeneration of phosphate in rabbit psoas muscle fibres. *J. Physiol. (Lond.).* 451:247–278.

Dantzig, J. A., M. G. Hibberd, D. R. Trentham, and Y. E. Goldman. 1991. Cross-bridge kinetics in the presence of MgADP investigated by photolysis of caged ATP in rabbit psoas muscle fibers. *J. Physiol. (Lond.).* 432:639–680.

Edman, K. A. P. 1979. The velocity of unloaded shortening and its relation to sarcomere length and isometric force in vertebrate muscle fibres. *J. Physiol. (Lond.).* 291:143–160.

Eisenberg, E., and W. W. Keilley. 1974. Troponin-tropomyosin complex. *J. Biol. Chem.* 249:4742–4748.

Ferenczi, M. A., Y. E. Goldman, and R. M. Simmons. 1984. The dependence of force and shortening velocity on substrate concentration in skinned muscle fibres from *Rana temporaria*. *J. Physiol. (Lond.).* 350: 519–543.

Fisher, A. J., C. A. Smith, J. B. Thoden, R. Smith, K. Sutoh, H. M. Holden, and I. Rayment. 1995a. Structural studies of myosin: nucleotide complexes: a revised model for the molecular basis of muscle contraction. *Biophys. J.* 68:19s–28s.

Fisher, A. J., C. A. Smith, J. B. Thoden, R. Smith, K. Sutoh, H. M. Holden, and I. Rayment. 1995b. X-ray structures of the myosin motor domain of *Dictyostelium discoideum* complexed with MgADPCBeF_x and MgADPCAlF_4^-. *Biochemistry.* 34:8960–8972.

Ford, L. E., A. F. Huxley, and R. M. Simmons. 1977. Tension responses to sudden length change in stimulated from muscle fibres near slack length. *J. Physiol. (Lond.).* 269:441–515.

Fortune, N. S., M. A. Geeves, and K. W. Ranatunga. 1991. Tension responses to rapid pressure release in glycerinated rabbit muscle fibers. *Proc. Natl. Acad. Sci. USA.* 88:7323–7327.

Goldman, Y. E., M. G. Hibberd, and D. R. Trentham. 1984. Relaxation of rabbit psoas muscle fibres from rigor by photochemical generation of adenosine-5′-triphosphate. *J. Physiol. (Lond.).* 354:577–604.

Goldman, Y. E., and R. M. Simmons. 1984. Control of sarcomere length in skinned muscle fibres of *Rana temporaria* during mechanical transients. *J. Physiol. (Lond.).* 350:497–518.

Harada, Y., K. Sakurada, T. Aoki, D. D. Thomas, and T. Yanadida. 1990. Mechanochemical coupling in actomyosin energy transduction studied by in vitro motility assay. *J. Mol. Biol.* 216:49–68.

Hibberd, M. G., J. A. Dantzig, D. R. Trentham, and Y. E. Goldman. 1985. Phosphate release and force generation in skeletal muscle fibers. *Science.* 228:1317–1319.

Higuchi, H., and S. Takemori. 1989. Butanedione monoxime suppresses contraction and ATPase activity of rabbit skeletal muscle. *J. Biochem.* 105:638–643.

Homsher, E., J. Lacktis, and M. Regnier. 1997. Strain-dependent modulation of phosphate transients in rabbit skeletal muscle fibers. *Biophys. J.* 72:1780–1792.

Homsher, E., and N. C. Millar. 1990. Caged compounds and striated muscle contraction. *Annu. Rev. Physiol.* 52:875–96.

Homsher, E., M. Regnier, and S. Tejeda. 1993. The effect of ATP analogues (NTP) on thin filament movement in motility assays and on the phosphate transient in rabbit glycerinated muscle fibers. *Biophys. J.* 64:A250.

Homsher, E., F. Wang, and J. R. Sellers. 1992. Factors affecting movement of F-actin filaments propelled by skeletal muscle heavy meromyosin. *Am. J. Physiol.* 262:C714–C722.

Johnson, K. A., and E. W. Taylor. 1978. Intermediate states of subfragment 1 and actosubfragment 1 ATPase: re-evaluation of the mechanism. *Biochemistry.* 17:3432–3442.

Keilley, W. W., H. M. Kalckar, and L. B. Bradley. 1956. The hydrolysis of purine and pyrimidine nucloeside triphosphates by myosin. *J. Biol. Chem.* 219:95–101.

Kron, S. J., and J. A. Spudich. 1986. Fluorescent actin filaments move on myosin fixed to a glass surface. *Proc. Natl. Acad. Sci. USA.* 83: 6272–6276.

Ma, Y. A., and E. W. Taylor. 1994. Kinetic mechanism of myofibril ATPase. *Biophys. J.* 66:1542–1553.

Margossian, S. S., and S. Lowey. 1982. Preparation of myosin and its subfragments from rabbit skeletal muscle. *Methods Enzymol.* 85:55–71.

Martyn, D. A., and A. M. Gordon. 1992. Force and stiffness in glycerinated rabbit psoas fibers: effects of calcium and elevated phosphate. *J. Gen. Physiol.* 99:795–816.

Millar, N. C., and E. Homsher. 1990. The effect of phosphate and calcium on force generation in glycerinated rabbit skeletal muscle fibers. *J. Biol. Chem.* 265:20234–20240.

Millar, N. C., and E. Homsher. 1992. Kinetics of force generation and phosphate release in skinned rabbit soleus muscle fibers. *Am. J. Physiol.* 262:C1239–C1245.

Pate, E., K. Franks-Skiba, H. White, and R. Cooke. 1993. The use of differing nucleotides to investigate cross-bridge kinetics. *J. Biol. Chem.* 268:10046–10053.

Pate, E., K. L. Nakamaye, K. Franks-Skiba, R. G. Yount, and R. Cooke. 1991. Mechanics of glycerinated muscle fibers using nonnucleoside triphosphate substrates. *Biophys. J.* 59:598–605.

Regnier, M., P. Bostani, and E. Homsher. 1993. The effect of ATP analogues (NTP) on isometric force and unloaded shortening velocity (V_{max}) in rabbit glycerinated muscle fibers. *Biophys. J.* 64:A250.

Regnier, M., and E. Homsher. 1996. The effect of NTP binding, cleavage rates, and cleavage equilibrium constants on mechanical behavior of the single rabbit skeletal muscle fiber at 10°C. *Biophys. J.* 70:A290.

Regnier, M., and E. Homsher. 1998. The effect of ATP analogues on post-hydrolytic and force development steps in skinned skeletal muscle fibers. *Biophys. J.* 74:2005–2015.

Regnier, M., D. A. Martyn, C. J. Freitag, and P. B. Chase. 1997. Inhibition of contraction by beryllium fluoride in skinned fibers from rabbit psoas muscle. *Biophys. J* 72:A379.

Regnier, M., C. Morris, and E. Homsher. 1995. Regulation of cross-bridge transition from a weakly to strongly bound state in skinned rabbit skeletal muscle fibers. *Am. J. Physiol.* 269:C1532–C1539.

Shimizu, T., K. Furusawa, S. Ohashi, Y. Y. Toyoshima, M. Okuno, G. Malik, and R. D. Vale. 1991. Nucleotide specificity of the enzymatic and motile activities of dynesin, kinesin, and heavy meromyosin. *J. Cell Biol.* 112:1189–1197.

Siemankowski, R. F., M. O. Wiseman, and H. D. White. 1985. ADP dissociation from actomyosin subfragment 1 is sufficiently slow to limit the unloaded shortening velocity in vertebrate muscle. *Proc. Natl. Acad. Sci. USA.* 82:658–662.

Sleep, J. A., and R. L. Hutton. 1980. Exchange between inorganic phosphate and adenosine 5′-triphosphate in the medium by actomyosin subfragment 1. *Biochemistry.* 19:1276–1283.

Toyoshima, Y. Y., S. J. Kron, E. M. McNally, K. R. Niebling, C. Toyoshima, and J. A. Spudich. 1987. Myosin subfragment-1 is sufficient to move actin filaments in vitro. *Nature.* 328:536–539.

Walker, J. W., Z. Lu, and R. L. Moss. 1992. Effects of Ca^{2+} on the kinetics of phosphate release in skeletal muscle. *J. Biol. Chem.* 267:2459–2466.

Weber, A. 1969. Parallel response of myofibrillar contraction and relaxation to four different nucleoside triphosphates. *J. Gen. Physiol.* 53: 781–791.

White, H. D. 1982. Special instrumentation and techniques for kinetic studies of contractile systems. *Methods Enzymol.* 85:698–708.

White, H. D., B. Belknap, and W. Jiang. 1993. Kinetics of binding and hydrolysis of a series of nucleoside triphosphates by actomyosin-S1. *J. Biol. Chem.* 268:10039–10045.

White, H., B. Belknap, and M. Webb. 1997. Kinetics of nucleoside triphosphate cleavage and phosphate release steps by associated rabbit skeletal actomyosin, measured using a novel fluorescent probe for phosphate. *Biochemistry.* 36:11828–11836.

White, H. D., and E. W. Taylor. 1976. Energetics and mechanism of actomyosin adenosine triphosphatase. *Biochemistry.* 15:5818–5826.

Woledge, R. C., N. A. Curtin, and E. Homsher. 1985. Energetic aspects of muscle contraction. *Monogr. Physiol. Soc.* 41:1–357.